Cell Biol Toxicol (2009) 25:379–391
DOI 10.1007/s10565-008-9092-8

Role of PARP-1 and PARP-2 in the expression of apoptosis-regulating genes in HeLa cells

Odile Cohausz · Felix R. Althaus

Received: 22 February 2008 / Accepted: 30 May 2008 / Published online: 28 June 2008

Abstract Poly (ADP-ribose) polymerase-1 (PARP-1) is a DNA-binding enzyme involved in DNA damage processing, apoptosis, and genetic stability. Many lines of evidence suggest that PARP-1 is implicated in transcriptional regulation of various genes through the modulation of chromatin structure or through direct interaction with transcription factors and/or transcription factor-binding sites. In the present study, we applied TaqMan Low-Density Array analyses to investigate the expression of genes involved in apoptotic cell death induced by an alkylating agent. Using RNA interference, we determined the roles of PARP-1 and PARP-2 in transcriptional regulation during apoptosis in HeLa cells. Of the 93 genes monitored, 33 differentially expressed genes were identified after induction of apoptosis. Whereas the down-regulation of PARP-1 and PARP-2 had no impact on gene expression per se, we observed that Bcl10, c-Rel, and tumor necrosis factor-related apoptosis-inducing ligand receptor-1 and -2 are differentially expressed after induction of apoptosis in a PARP-1-dependent manner. These findings suggest that PARP-1—but not PARP-2—is required for proper expression of major genes involved in regulation of apoptosis.

O. Cohausz · F. R. Althaus (✉)
Institute of Pharmacology and Toxicology,
University of Zurich-Vetsuisse,
Winterthurerstrasse 260,
CH-8057 Zurich, Switzerland
e-mail: fra@vetpharm.uzh.ch

Keywords Bcl10 · c-Rel · MNNG · RNA interference · TaqMan Low-Density Array · TRAIL

Abbreviations

ACTB	beta-actin
Bcl10	B-cell lymphoma 10
DMEM	Dulbecco's modified Eagle's medium
FBS	fetal bovine serum
GAPDH	glyceraldehyde-3-phosphate dehydrogenase
MNNG	*N*-methyl-*N*′-nitro-*N*′-nitrosoguanidine
PAR	poly(ADP-ribose)
PARP-1	PAR polymerase 1
PARP-2	PAR polymerase 2
RNAi	RNA interference
siRNA	small interfering RNA
TLDA	TaqMan® Low-Density Array
TRAIL-R1 and -R2	TNF-related apoptosis-inducing ligand receptor-1 and -2

Introduction

In response to DNA damage, poly(ADP-ribose) polymerase-1 (PARP-1) acts as a DNA nick sensor and is activated by DNA breaks to cleave NAD^+ to nicotinamide and adenosine diphosphate (ADP)-ribose.

Thereby, long branched poly(ADP-ribose) polymers (PAR) are synthesized and covalently attached to nuclear acceptor proteins, including PARP-1 itself (Schreiber et al. 2006). Several lines of evidence support a role of PARP-1 and PAR in the regulation of gene expression, and at least two mechanisms of transcriptional regulation have been described: (1) PARP-1 can directly modify structural proteins that constitute chromatin, and (2) PARP-1 functions as an enhancer/promoter-binding cofactor that can act in conjunction with other transcription-related factors (D'Amours et al. 1999; Hassa and Hottiger 2002; Haince et al. 2006). PARP-1 exerts its effects in modulating chromatin by directly (ADP-ribosyl)ating core histones and chromatin-associated proteins, thereby promoting the dissociation of nucleosomes and the decondensation of higher-order chromatin (D'Amours et al. 1999). The polyanionic PAR can act as a local matrix for core histones released from destabilized nucleosomes, providing further access to DNA (Althaus 1992; Realini and Althaus 1992). One example of histone-modifying PARP-1 activity is puff formation in *Drosophila* polytene chromosomes, which presents PARP-1-dependent accumulation of PAR at decondensed, transcriptionally active loci (Tulin and Spradling 2003). Activation of transcription was also shown to be induced by a histone H1 high-mobility group B exchange event triggered by PARP-1 activation, whereas on the other hand, the nucleosome-binding properties of PARP-1 were shown to promote the formation of transcriptionally repressed chromatin structures (Kim et al. 2004; Ju et al. 2006). Furthermore, recently Krishnakumar observed a reciprocal pattern of binding of histone H1 and PARP-1 at many RNA polymerase II-transcribed promoters that specifies transcriptional outcomes (Krishnakumar et al. 2008). With respect to the second mechanism of regulatory activity, the role of PARP-1 in transcription by directly altering the activity of enhancers and promoters is well-established. The PARP-1 regulatory effect at enhancers and promoters occurs in large part by functional interaction between PARP-1 and various non-histone proteins. Thereby, PARP-1 enzymatic activity is necessarily required for its transcription-regulating functions in some cases, whereas it is not needed in others (Kraus and Lis 2003). Several studies revealed that PARP-1 promotes activator-dependent transcription by interacting with RNA polymerase II-associated factors (Butler and Ordahl 1999), transcription enhancer factor 1 (TEF1), and a large number of transcription factors including AP-2, b-Myb, YY-1, Oct-1, NF-κB, and p53 (Oei et al. 1997; Nie et al. 1998; Kannan et al. 1999; Oliver et al. 1999; Cervellera and Sala 2000; Hassa et al. 2003; Wesierska-Gadek et al. 2003). As a co-repressor, PARP-1 modulates the expression of RXR-regulated genes (Miyamoto et al. 1999) and of a mu opioid receptor gene (Choi et al. 2008), as well as of the PARP-1 gene itself (Soldatenkov et al. 2002). In addition, Ju et al. (2004) identified PARP-1 as a component of a regulatory circuit, in which it plays a dual role as a component of a repressive complex that is also essential for gene activation.

Although less well described, other PARP family members also contribute to transcriptional regulation (Schreiber et al. 2006). Among the members of the PARP gene family characterized so far, PARP-2 shows the highest homology with the catalytic domain of PARP-1 and contributes, although to a lesser extent, to the formation of ADP-ribose polymers in response to DNA damage (Ame et al. 1999; Hassa et al. 2006). PARP-2 interacts with thyroid transcription factor-1 (TTF1) and regulates the expression of surfactant protein-B in lungs (Maeda et al. 2006).

In the present study, we used RNA interference (RNAi) in human cells to selectively down-regulate PARP-1 and PARP-2 in order to determine their individual contribution to apoptotic cell death at the transcriptional level. We chose a low-dose (50 μM) *N*-methyl-*N*′-nitro-*N*′-nitrosoguanidine (MNNG) treatment that triggers apoptotic cell death in HeLa cells as previously described (Cohausz et al. 2008). This type of cell death involves moderate activation of PAR synthesis, moderate changes in the ADP/ATP ratio of cells, activation of caspases-7 and -9, proteolytic processing of PARP-1, and apoptosis-inducing factor translocation from mitochondria to the nucleus (Cohausz et al. 2008). Furthermore, we showed that PARP-1, but not PARP-2, acts as pro-apoptotic factor, as knockdown of PARP-1—but not PARP-2—led to a significant increase in cell survival after MNNG treatment in comparison to control cells (Cohausz et al. 2008). In the present study, the expression patterns of 93 marker genes involved in the apoptosis pathway were investigated using the TaqMan Low-Density Array (TLDA) technique. Our results suggest

that, of the two tested PARP enzymes, only PARP-1 is involved in the regulation of major players of the apoptosis pathway, namely Bcl10, c-Rel, and tumor necrosis factor (TNF)-related apoptosis-inducing ligand receptor-1 and -2 (TRAIL-R1, TRAIL-R2), whereas the transcription of genes of the apoptosis pathway was not affected by RNAi-mediated silencing of PARP-2.

Materials and methods

Cell culture

All media and supplements used for cell culturing were obtained from GIBCO (Invitrogen, Basel, Switzerland). Human cervical carcinoma cells (HeLa S3) were cultured at 37°C in a water-saturated 5% CO_2/95% air atmosphere, in Dulbecco's modified Eagle's medium (DMEM) containing 4,500 mg/l glucose and supplemented with 10% (*v*/*v*) fetal bovine serum and antibiotics (complete DMEM).

Synthesis of siRNAs (small interfering RNAs) and transfection

Small interfering RNAs (siRNAs) were synthesized in vitro from oligonucleotide templates (Microsynth, Balgach, Switzerland) using a siRNA construction kit (Ambion), according to manufacturer's instructions. Purified siRNAs were dissolved in water at a concentration of 20 μM and stored at −80°C until use. As target for RNAi, 21 nucleotide sequences in the human coding region of PARP-1 (siRNA-P1-I, 5′-AAGAGCGAT GCCTATTACTGC-3′) and PARP-2 (siRNA-P2, 5′-AAGATGATGCCAGAGGAACTC-3′) cDNA were chosen as previously described (Cohausz et al. 2008). A scrambled version of siRNA was also synthesized and used as a negative control. For PARP-1 down-regulation assays, an additional siRNA specific for human PARP-1 (siRNA-P1-II, 5′-CAUCGAGGUG GCCUACAGU-3′) was designed and obtained from Microsynth. Cells were grown to 50–70% confluence in six-well plates and transfected with siRNAs at a final concentration of 80 nM in 1,000 μl OptiMEM, using siPORT Amine (Ambion) as the transfection reagent. After incubation for 4 h at 37°C, medium was changed to 3 ml per well complete DMEM, and cells were allowed to grow for 30 h.

MNNG treatment

Thirty hours after transfection with siRNA, cells were harvested by trypsinization, resuspended in complete DMEM and seeded into six-well plates. MNNG was dissolved in dimethyl sulfoxide at 2.0 M and diluted in complete DMEM to a final dilution of 50 μM just before use. After attachment of cells to the bottom of the plates, complete DMEM containing MNNG was added to exponentially growing cells in six-well plates, and cells were incubated at 37°C for 6 h.

RNA extraction and reverse transcription

Total RNA was isolated from untreated HeLa cells and from HeLa cells treated with 50 μM MNNG for 6 h. Cells were washed with phosphate-buffered saline (PBS) and lysed directly in the lysis buffer from RNeasy® Mini Kit (QIAGEN, Hilden, Germany). Lysates were homogenized using a QIAshredder® spin column (QIAGEN), and total RNA was isolated with ion exchange spin columns (QIAGEN RNeasy® Mini Kit; QIAGEN). Total RNA (1.5 μg) was converted to single-stranded cDNA using the High-Capacity cDNA Reverse Transcription Kit with RNase Inhibitors according to the manufacturer (Applied Biosystems, Foster City, CA, USA).

mRNA gene analyses by quantitative reverse transcriptase polymerase chain reaction

Predesigned TaqMan Low-Density Arrays (96 TaqMan® Gene Expression assay preconfigured in a 384-well format, Part no. 437816, microfluidic cards; Applied Biosystems), were used in a two-step reverse transcriptase polymerase chain reaction (RT-PCR) process using the ABI Prism 7900HT Sequence Detection System (Applied Biosystems) with a TaqMan Low-Density Array Upgrade (Applied Biosystems). Each cDNA sample (100 μl) was added to an equal volume of 2× TaqMan Universal PCR Master Mix (Applied Biosystems). After gentle mixing, the solution was transferred into a loading port on a TLDA card (Applied Biosystem). Each of the samples were analyzed in a single TLDA run with each of the four TLDA experiments running on separate cards using an Applied Biosystems 7900 HT Fast-Real-Time PCR System. Thermal cycler conditions were as follows: 2 min at 50°C, 10 min at

94.5°C and 30 s at 97°C, and 1 min at 59.7°C for 40 cycles. Data acquisition was done according to the manufacturer's suggestions. Quantitative real-time PCR amplification of single genes was performed with specifically designed primers (Assay-on-demand Gene Expression products, Applied Biosystems) using an ABI PRISM 7700 cycler, at the default setting program (95°C, 15 s; 60°C, 1 min; 40 cycles). TaqMan gene expression assays (Applied Biosystems) for Bcl10 (assay ID Hs00961847_m1), c-Rel (assay ID Hs00968436_m1), PARP-1 (assay ID Hs00242302_m1), PARP-2 (assay ID Hs Hs00193931_m1), TRAIL-R1 (assay ID Hs00269492_m1) and TRAIL-R2 (assay ID Hs00366272_m1), were used for quantification of mRNA expression of the respective genes. The expression of three potential housekeeping genes was measured in cDNA from siRNA-C and siRNA-P1-I samples in the absence and presence of MNNG. Glyceraldehydes-3-phosphate dehydrogenase (GAPDH) showed a good average expression stability (<0.2) and was selected as single housekeeping gene using the software geNorm (Vandesompele et al. 2002). Another internal control gene, beta-actin (ACTB), was used for validation of results. For analysis, expression levels of target genes were normalized to GAPDH and ACTB. Gene expression values were then calculated based on the $\Delta\Delta C_t$ method, with data normalized to untreated controls (siRNA-C). Relative quantities (RQ) were determined using the equation: $RQ = 2^{-\Delta\Delta Ct}$. Only genes with reproducible amplification curves of quadruplicate determinations were analyzed and presented.

Statistical analyses

Data are expressed as mean±SD. All statistical analyses were conducted with NCSS (NCSS, Statistical & Power Analysis Software, Utah, USA). For statistical analyses, a one-sample *t* test or a Kruskal–Wallis test was used as indicated. The analyses were two-tailed, and *p* values <0.05 were considered statistically significant.

Western blot analyses

Cells were washed with ice-cold PBS and then harvested directly in Laemmli buffer (60 mM Tris–HCl, pH 6.8, 2% sodium dodecyl sulfate (SDS), 2% 2-mercaptoethanol, 8% glycerol, 0.0025% bromphenol blue), sonicated and incubated for 1 min at 95°C. Soluble proteins were collected in the supernatants after centrifugation, separated by electrophoresis on SDS-polyacrylamide gels, and finally electroblotted on polyvinylidene fluoride membranes (Bio-Rad, Hercules, CA, USA). Blots were probed with monoclonal anti-α-tubulin (Sigma, Buchs, Switzerland; 1:5,000), polyclonal anti-Bcl10 (Cell Signaling Technology, MA, USA; 1:1,000), polyclonal anti-cleaved caspase-7 (Cell Signaling Technology; 1:1,000), polyclonal anti-cleaved caspase-9 (Cell Signaling Technology; 1:1,000), polyclonal anti-c-Rel (Cell Signaling Technology; 1:1,000), monoclonal anti-GAPDH (Ambion; 1:80,000), monoclonal anti-PARP-1 (Alexis, Lausen, Switzerland; c2–10; 1:5,000), polyclonal anti-PARP-1 p85 fragment (Promega, Madison, WI, USA; 1:500), monoclonal anti-PARP-2 (Alexis; 4G8; 1:50), polyclonal anti-TRAIL-R1 (Millipore, MA, USA; 1:1,000), polyclonal anti-TRAIL-R2 antibodies (Millipore; 1:500), and monoclonal anti-α-tubulin antibodies (Sigma; 1:5,000) in succession. Immunodetection was performed by enhanced chemiluminescense (PIERCE, Rockford, IL, USA, ECL detection kit). Images were acquired by exposure to autoradiographic films and by Luminescent Image Analyzer (LAS-3000, Fujifilm, Switzerland).

Results

Gene expression profile of MNNG-treated HeLa cells Based on dose- and time-finding experiments,

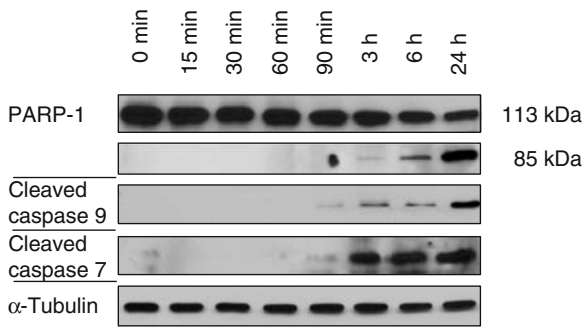

Fig. 1 Western blot analysis of caspase-dependent cleavage of PARP-1 as well as activated caspase-7 and caspase-9 after MNNG-induced cell death. Cells were treated with 50 μM for indicated time points. Immunoblotting of whole cell lysates was performed with antibodies detecting the full-length form and the 85-kDa fragment of PARP-1, as well as cleaved caspase-7 and caspase-9

Table 1 mRNA profile of HeLa cells (siRNA-C and siRNA-P1-I) 6 h after treatment with MNNG

	siRNA-C	siRNA-P1-I	Gene name	Gene description
Accession number	Fold change			
Bcl-2 family-regulated pathway				
NM003921.3	−1,0	*2,1*	BCL10	B-cell CLL/lymphoma 10
NM015367.2	*−1,5*	−1,3	BCL2L13	BCL2-like 13 (apoptosis facilitator)
NM004050.2	*−1,8*	−1,7	BCL2L2	BCL2-like 2
NM000633.2	*−3,1*	−2,5	BCL2	B-cell CLL/lymphoma 2
NM207002.2	*1,8*	*2,7*	BCL2L11	BCL2-like 11 (apoptosis facilitator)
NM021127.2	*3,0*	*7,4*	PMAIP1	Phorbol-12-myristate-13-acetate-induced protein 1
NM001197.3	*7,0*	7,1	Bik	Bcl2-interacting killer
CARD family				
NM006092.1	*−1,8*	*−1,6*	CARD4	Caspase recruitment domain-containing protein 4
NM033004.3	*−1,9*	−1,4	NALP1	NLR family, pyrin domain containing 1
NM181861.1	*−3,5*	−2,5	APAF1	Apoptotic peptidase activating factor 1
IAP family				
NM001166.3	*−1,7*	−1,1	BIRC2	Baculoviral IAP repeat-containing 2
NM001167.2	*−3,2*	−2,3	BIRC4	Baculoviral IAP repeat-containing 4
NM182962.1	*−3,3*	−1,4	BIRC3	Baculoviral IAP repeat-containing 3
NM016252.3	*−4,2*	−4,4	BIRC6	Baculoviral IAP repeat-containing 6
NM004536.2	*9,6*	5,9	BIRC1	Baculoviral IAP repeat-containing 1
NF-κB signaling pathway				
NM001556.1	*−1,6*	−1,5	IKBKB	Inhibitor of kappa light polypeptide gene enhancer in B-cells, kinase beta
NM014002.2	*−1,8*	*−2,0*	IKBKE	Inhibitor of kappa light polypeptide gene enhancer in B-cells, kinase epsilon
NM003998.2	*−2,2*	−1,6	NFKB1	Nuclear factor of kappa light polypeptide gene enhancer in B-cells 1 (p105)
NM013254.2	*−2,2*	−1,2	TBK1	TANK-binding kinase 1
NM001278.3	*−2,3*	−1,2	CHUK	Conserved helix-loop-helix ubiquitous kinase
NM002908.2	*−2,4*	1,5	c-Rel	v-rel reticuloendotheliosis viral oncogene homolog (avian)
NM021975.2	1,0	*1,6*	RelA	v-rel reticuloendotheliosis viral oncogene homolog A, nuclear factor of kappa light polypeptide gene enhancerin B-cells 3, p65
NM139239.1	*2,1*	1,7	TA-NFKBH	T-cell activation NFKB-like protein
NM002529.2	*2,7*	*2,3*	NFKBIA	Nuclear factor of kappa light polypeptide gene enhancer in B-cells inhibitor, alpha
NM031419.2	*2,8*	*2,2*	NFKBIZ	Nuclear factor of kappa light polypeptide gene enhancer in B-cells inhibitor, zeta
TNF receptor pathway				
NM003844.2	*−1,6*	1,2	TRAIL-R1	TNF-related apoptosis inducing ligand receptor 1
NM147187.1	*−1,6*	1,2	TRAIL-R2	TNF-related apoptosis inducing ligand receptor 2
NM014452.3	*−1,6*	1,3	TNFRSF21	Tumor necrosis factor receptor superfamily, member 21
NM003804.3	*−1,7*	1,3	RIPK1	Receptor (TNFRSF)-interacting serine-threonine kinase 1
NM003790.2	*−1,8*	−2,0	TNFRSF25	Tumor necrosis factor receptor superfamily, member 25
NM003879.3	*−1,9*	−1,2	CFLAR	CASP8 and FADD-like apoptosis regulator
NM000595.2	*3,1*	4,3	LTA	Lymphotoxin alpha (TNF superfamily, member 1)
NM000594.2	*3,6*	2,2	TNF	TNF superfamily, member 2
Others				
NM005338.4	*−1,9*	−2,3	HIP1	Death effector domain containing 2
NM032991.2	−1,0	1,3	Casp3	Caspase 3
NM003768.2	−1,1	*2,0*	PEA15	Phosphoprotein enriched in astrocytes 15
NM021960.3	1,1	*2,3*	Mcl1	Myeloid cell leukemia sequence 1 (BCL2-related)
NM133328.2	*1,6*	1,4	DEDD2	Death effector domain containing 2

Significant transcripts are indicated in italics, $p<0.05$; siRNA-C: unpaired t test; siRNA-P1: Kruskal–Wallis test.

50 μM concentrations of MNNG and a treatment period of 6 h were used in all subsequent experiments. Dose-finding experiments are shown in Figure S2 of our previous paper (Cohausz et al. 2008) which is available under http://www.vetpharm.uzh.ch/suppl/cohausz_et_al_S2.pdf. The time optimum was defined at 6 h after MNNG treatment. At this time point, we observed a marked increase of the caspase cleavage fragment of PARP-1, a hallmark of apoptosis, as well as cleavage of caspase-7 and -9, indicating apoptotic cell death (Fig. 1).

The transcriptional profiles of a broad set of genes of the apoptosis pathway were examined by TLDA containing 93 apoptosis-related genes to assess the effects of the alkylating agent MNNG on gene expression. Genes whose expression was significantly up- or down-regulated in MNNG-treated cells are listed in Table 1. In HeLa cells, 36% (33 of 93) of genes showed significant differences in the expression level ($p<0.05$, unpaired t test) after MNNG treatment. Thereby, the expression of 22 genes (24%) was down-regulated (by a factor of 1.5 to 4.2), and that of 11 genes (12%) was up-regulated (by a factor of 1.6 to 9.6). Of the 33 genes that had altered expression as a result of treatment with the alkylating agent, those involved in the Bcl-2 family-regulated pathway, the NF-κB signaling pathway, and the TNF receptor pathway as well as genes of the caspase recruitment domain (CARD) and inhibitor of apoptosis (IAP) family were found (Table 1). In addition, the transcriptional profiles of PARP-1 knock-down cells after MNNG treatment is shown in Table 1. For comparison of fold change between the two housekeeping genes, GAPDH and ACTB, scatter plots of the transcriptional profiles of control as well as PARP-1 knock-down cells after MNNG treatment were generated (Fig. 2). The data set obtained after normalization to GAPDH showed good correlation with ACTB data with R^2 values of 0.90 and 0.98 for control and PARP-1 knock-down cells, respectively.

Suppression of PARP-1 and PARP-2 by siRNA technique We knocked down the expression of either PARP-1 or PARP-2 by use of RNA interference as previously described (Cohausz et al. 2008). As shown in Fig. 3a, transfection of HeLa cells with two different siRNA constructs specific for PARP-1 (siRNA-P1-I and siRNA-P1-II), but not with control siRNA (siRNA-C), significantly suppressed the expression of PARP-1 m-RNA. Western blot analyses of PARP-1 protein expression in the cell homogenates utilizing an anti-PARP-1 antibody confirmed a significant decrease in PARP-1 protein levels at 52 h after transfection (Fig. 3a). Likewise, after knock-down of PARP-2 by RNAi, the expression of PARP-2 m-RNA and protein level were reduced compared with that of siRNA-C transfected cells (Fig. 3b).

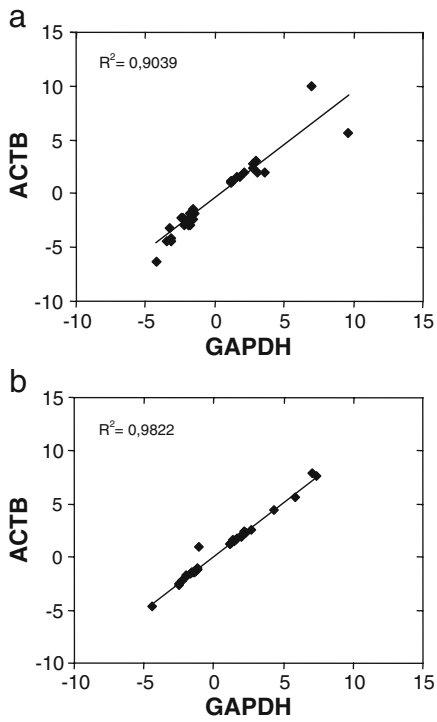

Fig. 2 Correlation of fold change after MNNG treatment of siRNA-C (**a**) and siRNA-P1-I (**b**) transfected HeLa cells determined by normalization to GAPDH and ACTB. *y-Axis*, fold change determined by normalization to ACTB; *x-axis*, fold change determined by normalization to GAPDH. A *trend line* and the corresponding R^2 value are presented in each plot

Analysis of the effects of PARP-1 and PARP-2 deficiency on gene expression To assess the effect of either PARP-1 or PARP-2 deficiency on gene expression, we examined the transcriptional profiles of PARP-1-siRNA- as well as PARP-2-siRNA-transfected HeLa cells in comparison to control cells by TLDA. Under basal conditions, PARP-1-, as well as PARP-2-down-regulated cells, showed no significant changes in the expression of genes of the apoptosis pathway (data not shown). By contrast, after MNNG treatment, we observed significant changes in the expression of major

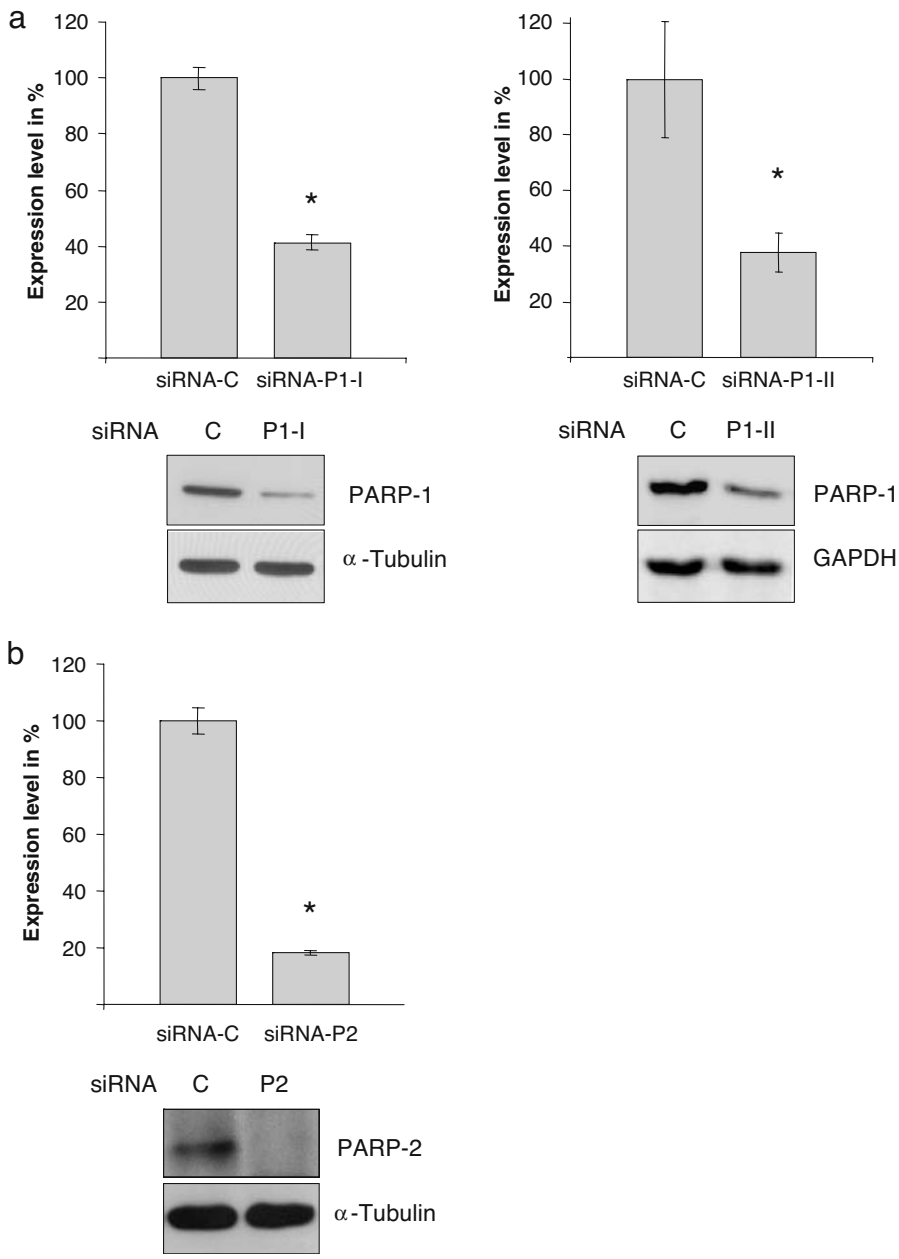

Fig. 3 Specific knockdown of PARP-1 and PARP-2 by RNA interference. Relative fold changes of PARP-1 (siRNA-P1-I and siRNA-P1-II; **a**) and PARP-2 (siRNA-P2; **b**) expression detected by real-time RT-PCR and Western blot analysis 2 days after transfection with siRNA. For real-time RT-PCR experiments, the results of at least three independent experiments with triplicate determinations are summarized. *Error bars* indicate mean±SD in percent of control (*$p<0.05$, unpaired *t* test)

genes of the apoptosis pathway, namely, Bcl10, c-Rel, TRAIL-R1, and TRAIL-R2, in PARP-1-silenced cells in comparison to control cells after normalization to GAPDH (Fig. 4a) and ACTB (Fig. 4b). The expression of Bcl10 was 2.0-fold up-regulated in PARP-1-down-regulated cells after MNNG treatment (siRNA-P1-I, +MNNG) in comparison to treated control cells (siRNA-C, +MNNG; Fig. 4a). We also observed significant differences of Bcl10 expression between untreated and MNNG-treated PARP-1-down-regulated cells. Furthermore, the three transcripts c-Rel, TRAIL-R1, and TRAIL-R2 were significantly up-regulated 3.1-, 2.1- and 2.0-fold in PARP-1-down-regulated cells after MNNG treatment (siRNA-P1-I, +MNNG) in comparison to treated control cells (siRNA-C, +MNNG; Fig. 4a). Thereby, the initial decrease in the expression of these genes induced by MNNG treatment of siRNA-C-transfected cells was abrogated. Moreover, knockdown of PARP-1 in MNNG-treated cells reversed this effect and led to an increase in gene expression of the

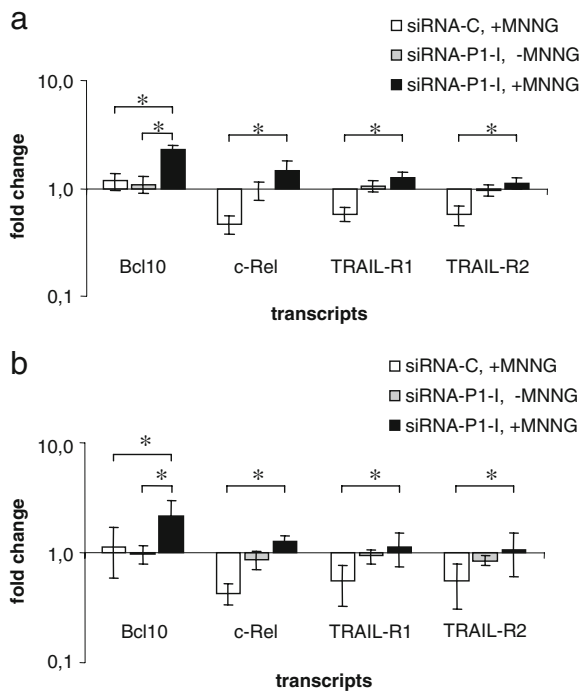

Fig. 4 Gene expression analysis of HeLa cells in the presence or absence of PARP-1. Shown are values of gene expression fold changes occurring after knock-down of PARP-1 (siRNA-P1-I) and treatment with MNNG in comparison to untreated siRNA-C-transfected control cells (set as 1). *Bars* illustrate mean values of four different TLDA experiments with standard deviation. Significant genes of a fold change of ≥2 are shown (*$p<0.05$, Kruskal–Wallis test). Data are normalized to GAPDH (**a**) and to ACTB (**b**), respectively

transcripts c-Rel, TRAIL-R1, and TRAIL-R2. After normalization to ACTB, Bcl10, c-Rel, TRAIL-R1, and TRAIL-R2 were significantly up-regulated 2.0-, 3.1-, 2.1-, and 2.0-fold, respectively, in PARP-1-down-regulated cells after MNNG treatment (siRNA-P1-I, +MNNG) in comparison to treated control cells (siRNA-C, +MNNG; Fig. 4b), which is consistent with the gene expression patterns observed after normalization to GAPDH (Fig. 4a).

In order to verify the results from the TLDA analyses, we compared these data with results obtained in single-gene real-time RT-PCR experiments for Bcl10, c-Rel, TRAIL-R1, and TRAIL-R2 (Fig. 5). To exclude off-target silencing effects mediated by specific siRNA, we employed two different sequences of PARP-1 (siRNA-P1-I and siRNA-P1-II) in these single-gene real-time RT-PCR analyses. Data were normalized either to GAPDH (Fig. 5a) or to ACTB (Fig. 5b). Consistent with the results of the TLDA analyses, a marked increase in transcript levels of Bcl10, c-Rel, TRAIL-R1, and TRAIL-R2 in PARP-1-down-regulated cells was observed by conventional real-time RT-PCR analyses of single genes using either of the PARP-1 siRNA sequences (siRNA-P1-I or siRNA-P1-II; Fig. 5a,b).

In contrast to these findings in PARP-1-silenced cells, we did not observe any significant changes in the expression of genes of the apoptosis pathway in PARP-2-down-regulated cells after MNNG treatment.

Up-regulated expression of specific proteins after PARP-1 down-regulation in MNNG-treated HeLa cells The aforementioned changes in the expression of specific genes observed by TLDA analyses and single-gene real-time RT-PCR experiments were verified at protein level by immunoblot analysis. Antibodies specific for Bcl10, c-Rel, TRAIL-R1, and TRAIL-R2 revealed an increase in protein expression for all four proteins in PARP-1-silenced cells treated with MNNG (siRNA-P1) in comparison to MNNG-treated control cells (siRNA-C; Fig. 6a). As shown in Fig. 6b, quantification of Western blot analyses confirmed increased protein levels that were 1.6-fold for Bcl10, 1.7-fold for c-Rel, 1.5-fold for TRAIL-R1, and 1.7-fold for TRAIL-R2.

Discussion

Recent reports have demonstrated several coregulator functions of PARP-1 as activator or co-repressor of transcription (Kraus and Lis 2003; Hassa et al. 2003; Ju et al. 2006; Haince et al. 2006). One study attests to a similar function of PARP-2 (Maeda et al. 2006). In the present study, we analyzed the contribution of the two enzymes by combining siRNA-mediated silencing with TaqMan Low-Density Arrays analyses, an array method that allows the simultaneous quantitative assessment of the gene expression profile of an entire pathway. Thereby, we focused on the roles of PARP-1 and PARP-2 in the apoptosis pathway. Dissecting the contribution of PARP-1 and PARP-2 by RNAi in living cells in the absence of DNA damage, we observed that neither of the enzymes is involved in the constitutive expression of apoptosis-related genes. By contrast, after induction of apoptosis by low doses of MNNG, our results of the TLDA analyses revealed four PARP-1-dependent genes,

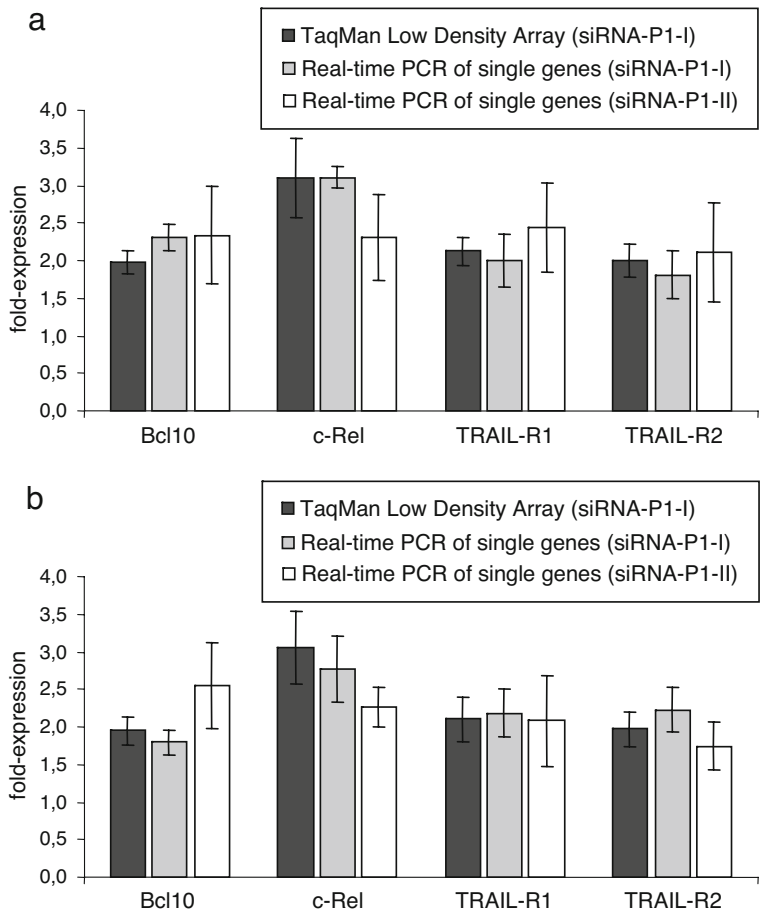

Fig. 5 Fold changes of indicated genes determined by TaqMan Low-Density Array and real-time PCR analyses. Shown are values of gene expression changes by PARP-1 down-regulation in MNNG-treated HeLa cells. *Bars* illustrate mean values of four independent TLDA experiments or four quantitative real-time PCR runs of single genes (triplicate measurements) of four independent experiments with standard deviation. Data are normalized to GAPDH (**a**) and to ACTB (**b**), respectively

whereas none was found to be PARP-2-dependent. We showed that the four transcripts of Bcl10, c-Rel, TRAIL-R1, and TRAIL-R2 were up-regulated 2.0-, 3.1-, 2.1-, and 2.0-fold, respectively, in PARP-1-down-regulated cells (Fig. 5). Furthermore, Bcl10, c-Rel, TRAIL-R1, and TRAIL-R2 protein levels were also found to be significantly up-regulated.

Although single genes such as GAPDH have often been used for normalization purposes in real-time RT-PCR experiments, expression of 'housekeeping' genes can vary (Vandesompele et al. 2002). We chose GAPDH and ACTB to verify that the results were independent of the reference gene selected. In addition, 'off-target' effects may be a problem in RNA interference experiments. Therefore, we present two sets of results, i.e., each normalized to GAPDH and to ACTB and each with two different siRNA sequences for PARP-1.

The transcription factor NF-κB is a homo- or hetero-dimeric complex made up of members of the Rel family of DNA binding proteins. In humans, this family is comprised of c-Rel, Rel B, p50, p52, and Rel A (p65; Karin and Lin 2002). NF-κB may play an anti-apoptotic (Beg and Baltimore 1996; Van Antwerp et al. 1996; Attar et al. 1998; Ravi et al. 2001) and a pro-apoptotic role (Abbadie et al. 1993; Lipton 1997; Ryan et al. 2000; Ravi et al. 2001). The c-Rel subunit of the transcription factor NF-κB has been shown to induce the expression of TRAIL-R1 and TRAIL-R2, whereas Rel A inhibits the expression of the receptors (Ravi et al. 2001; Chen et al. 2003). TRAIL-R1 and TRAIL-R2 are type I transmembrane proteins containing cytoplasmic sequences, termed 'death domains', recruiting adaptor proteins and activating caspases (Golstein 1997). Tumor-necrosis factor-related apoptosis-inducing ligand triggers apoptosis through engagement of the death receptors, TRAIL-R1 and TRAIL-R2. As we observed, concurrent to the up-regulation of c-Rel, TRAIL-R1, and TRAIL-R2 under apoptotic conditions in PARP-1-down-regulated cells, it is

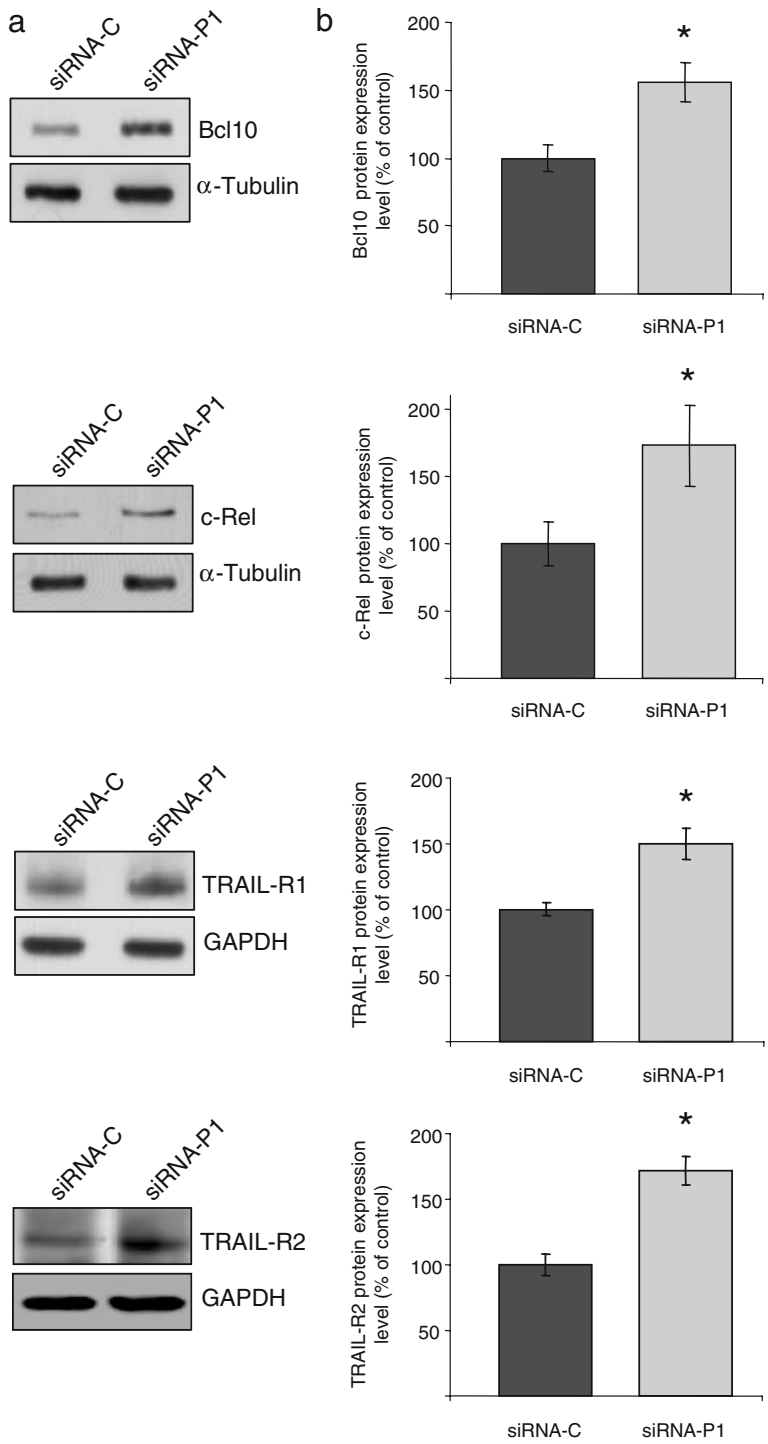

Fig. 6 Protein expression of specific genes involved in TRAIL-receptor signalling and NF-κB pathway after knockdown of PARP-1 in MNNG treated HeLa cells. Cell extracts of siRNA-C- and siRNA-P1-transfected cells were subjected to immunoblot analysis with antibodies detecting Bcl10, c-Rel, TRAIL-R1, and TRAIL-R2. Quantification of immunoblots was carried out by scanning densitometry of individual bands with ImageQuant software (Molecular Dynamics/GE Healthcare). *Error bars* indicate mean±SD in percent of control of at least four analyses (*$p<0.01$, unpaired *t* test)

likely that the induction of TRAIL-R1 and TRAIL-R2 was due to an increased expression of c-Rel. Intriguingly, TRAIL signaling does not only lead to the activation of effector caspases and subsequent initiation of apoptosis but can also induce non-apoptotic pathways, which includes the activation of NF-κB, PKB/Akt, and MAPKs (Falschlehner et al. 2007).

In addition to genes involved in the TRAIL signaling pathway, the expression of Bcl10 mRNA and protein levels were also significantly up-regulated in PARP-1-down-regulated cells after MNNG treatment. Bcl10 is a caspase recruitment domain-containing protein that was originally identified in mucous-associated lymphoid tissue lymphomas (MALT). Transient over-expression of wild-type Bcl10 in cell lines both induces apoptosis and activates NF-κB (Yan et al. 1999; Thome et al. 1999; Willis et al. 1999; Koseki et al. 1999). Although Bcl10 was initially shown to act as a pro-apoptotic factor, there are indications of an anti-apoptotic role of Bcl10 as well (Hosokawa 2005). Thereby, Bcl10/MALT-induced NF-κB activation may contribute to anti-apoptotic action probably through NF-κB-mediated up-regulation of apoptotic inhibitor genes (Hosokawa 2005).

Taken together, we observed that only PARP-1, and not PARP-2, is involved in transcriptional regulation of genes of the apoptosis pathway. Specific knockdown of PARP-1 led to an increase in transcription levels of major genes of the TRAIL pathway as well as of Bcl10, indicating that PARP-1 acts as a co-repressor of genes involved in the regulation of apoptosis pathways. Our previous paper showed that PARP-1, but not PARP-2, acts as a pro-apoptotic factor, as knockdown of PARP-1—but not PARP-2—led to a significant increase in cell survival after MNNG treatment in comparison to control cells (Cohausz et al. 2008). Due to the described dual functions (pro- and anti-apoptotic) of the transcripts Bcl10, TRAIL-R1, and TRAIL-R2, we suggest that the apoptotic response depends on the balance of apoptotic signals as mediated by caspases and anti-apoptotic programmes controlled by NF-κB favoring a pro-apoptotic role of PARP-1 in cell death induced by low doses of the alkylating agent MNNG.

The mechanism by which PARP-1 regulates the expression of Bcl10, c-Rel, TRAIL-R1, and TRAIL-R2 remains to be elucidated. Recent reports have shown that PARP-1 can bind sequence specifically to the promoter region of particular genes and affect the gene expression (Butler and Ordahl 1999; Akiyama et al. 2001; Nirodi et al. 2001; Zhang et al. 2002). In addition, PARP-1 interacts directly with a variety of transcription factors (Oei et al. 1997; Nie et al. 1998; Kannan et al. 1999; Oliver et al. 1999; Cervellera and Sala 2000; Hassa et al. 2003; Wesierska-Gadek et al. 2003) as well as it is involved in the modulation of chromatin structure (Haince et al. 2006). Another unanswered question is whether Bcl10 and c-Rel are direct targets of PARP-1 and whether the enzymatic activity of PARP-1 is required for their down-regulation. These aspects, as well as the question whether the observed phenomenon can be generalized for DNA damage and other cell types, are now subject of further studies about transcriptional control mechanisms in response to DNA damage.

Acknowledgements We thank Dr. Andreas Bergthaler and the Institute of Experimental Immunology, University Hospital Zurich, for providing access to an ABI PRISM 7900HT Sequence Detection System, and Prof. Dr. Markus Doherr, for assistance and helpful discussions with the statistical analyses. This work was supported by a grant from the Swiss National Foundation for scientific research awarded to F.R.A.

References

Abbadie C, Kabrun N, Bouali F, Smardova J, Stehelin D, Vandenbunder B, et al. High levels of c-rel expression are associated with programmed cell death in the developing avian embryo and in bone marrow cells in vitro. Cell 1993;75:899–912.

Akiyama T, Takasawa S, Nata K, Kobayashi S, Abe M, Shervani NJ, et al. Activation of Reg gene, a gene for insulin-producing beta-cell regeneration: poly(ADP-ribose) polymerase binds Reg promoter and regulates the transcription by autopoly(ADP-ribosyl)ation. Proc Natl Acad Sci U S A 2001;98:48–53.

Althaus FR. Poly ADP-ribosylation: a histone shuttle mechanism in DNA excision repair. J Cell Sci. 1992;102(Pt 4):663–70.

Ame JC, Rolli V, Schreiber V, Niedergang C, Apiou F, Decker P, et al. PARP-2, A novel mammalian DNA damage-dependent poly (ADP-ribose) polymerase. J Biol Chem. 1999;274:17860–8.

Attar RM, Macdonald-Bravo H, Raventos-Suarez C, Durham SK, Bravo R. Expression of constitutively active IkappaB beta in T cells of transgenic mice: persistent NF-kappaB activity is required for T-cell immune responses. Mol Cell Biol. 1998;18:477–87.

Beg AA, Baltimore D. An essential role for NF-kappaB in preventing TNF-alpha-induced cell death. Science 1996;274:782–4.

Butler AJ, Ordahl CP. Poly(ADP-ribose) polymerase binds with transcription enhancer factor 1 to MCAT1 elements to regulate muscle-specific transcription. Mol Cell Biol. 1999;19:296–306.

Cervellera MN, Sala A. Poly(ADP-ribose) polymerase is a B-MYB coactivator. J Biol Chem. 2000;275:10692–6.

Chen X, Kandasamy K, Srivastava RK. Differential roles of RelA (p65) and c-Rel subunits of nuclear factor kappa B in tumor necrosis factor-related apoptosis-inducing ligand signaling. Cancer Res. 2003;63:1059–66.

Choi HS, Hwang CK, Kim CS, Song KY, Law PY, Loh HH, et al. Transcriptional regulation of mouse mu opioid receptor gene in neuronal cells by Poly(ADP-ribose) polymerase-1. J Cell Mol Med. 2008 (in press).

Cohausz O, Blenn C, Malanga M, Althaus FR. The roles of poly(ADP-ribose)-metabolizing enzymes in alkylation-induced cell death. Cell Mol Life Sci. 2008;65(4):644–55.

D'Amours D, Desnoyers S, D'Silva I, Poirier GG. Poly(ADP-ribosyl)ation reactions in the regulation of nuclear functions. Biochem J. 1999;342(Pt 2):249–68.

Falschlehner C, Emmerich CH, Gerlach B, Walczak H. TRAIL signalling: decisions between life and death. Int J Biochem Cell Biol. 2007;39:1462–75.

Golstein P. Cell death: TRAIL and its receptors. Curr Biol. 1997;7:R750–3.

Haince JF, Rouleau M, Poirier GG. Transcription. Gene expression needs a break to unwind before carrying on. Science 2006;312:1752–3.

Hassa PO, Hottiger MO. The functional role of poly(ADP-ribose)polymerase 1 as novel coactivator of NF-kappaB in inflammatory disorders. Cell Mol Life Sci. 2002;59:1534–53.

Hassa PO, Buerki C, Lombardi C, Imhof R, Hottiger MO. Transcriptional coactivation of nuclear factor-kappaB-dependent gene expression by p300 is regulated by poly (ADP)-ribose polymerase-1. J Biol Chem. 2003;278:45145–53.

Hassa PO, Haenni SS, Elser M, Hottiger MO. Nuclear ADP-ribosylation reactions in mammalian cells: where are we today and where are we going? Microbiol Mol Biol Rev. 2006;70:789–829.

Hosokawa Y. Anti-apoptotic action of API2-MALT1 fusion protein involved in t(11;18)(q21;q21) MALT lymphoma. Apoptosis 2005;10:25–34.

Ju BG, Solum D, Song EJ, Lee KJ, Rose DW, Glass CK, et al. Activating the PARP-1 sensor component of the groucho/TLE1 corepressor complex mediates a CaMKinase IIdelta-dependent neurogenic gene activation pathway. Cell 2004;119:815–29.

Ju BG, Lunyak VV, Perissi V, Garcia-Bassets I, Rose DW, Glass CK, et al. A topoisomerase IIbeta-mediated dsDNA break required for regulated transcription. Science 2006;312:1798–802.

Kannan P, Yu Y, Wankhade S, Tainsky MA. PolyADP-ribose polymerase is a coactivator for AP-2-mediated transcriptional activation. Nucleic Acids Res. 1999;27:866–74.

Karin M, Lin A. NF-kappaB at the crossroads of life and death. Nat Immunol. 2002;3:221–7.

Kim MY, Mauro S, Gevry N, Lis JT, Kraus WL. NAD+-dependent modulation of chromatin structure and transcription by nucleosome binding properties of PARP-1. Cell 2004;119:803–14.

Koseki T, Inohara N, Chen S, Carrio R, Merino J, Hottiger MO, et al. CIPER, a novel NF kappaB-activating protein containing a caspase recruitment domain with homology to Herpesvirus-2 protein E10. J Biol Chem. 1999;274:9955–61.

Kraus WL, Lis JT. PARP goes transcription. Cell 2003;113:677–83.

Krishnakumar R, Gamble MJ, Frizzell KM, Berrocal JG, Kininis M, Kraus WL. Reciprocal binding of PARP-1 and histone H1 at promoters specifies transcriptional outcomes. Science 2008;319:819–21.

Lipton SA. Janus faces of NF-kappa B: neurodestruction versus neuroprotection. Nat Med. 1997;3:20–2.

Maeda Y, Hunter TC, Loudy DE, Dave V, Schreiber V, Whitsett JA. PARP-2 interacts with TTF-1 and regulates expression of surfactant protein-B. J Biol Chem. 2006;281:9600–6.

Miyamoto T, Kakizawa T, Hashizume K. Inhibition of nuclear receptor signalling by poly(ADP-ribose) polymerase. Mol Cell Biol. 1999;19:2644–9.

Nie J, Sakamoto S, Song D, Qu Z, Ota K, Taniguchi T. Interaction of Oct-1 and automodification domain of poly(ADP-ribose) synthetase. FEBS Lett 1998;424:27–32.

Nirodi C, NagDas S, Gygi SP, Olson G, Aebersold R, Richmond A. A role for poly(ADP-ribose) polymerase in the transcriptional regulation of the melanoma growth stimulatory activity (CXCL1) gene expression. J Biol Chem. 2001;276:9366–74.

Oei SL, Griesenbeck J, Schweiger M, Babich V, Kropotov A, Tomilin N. Interaction of the transcription factor YY1 with human poly(ADP-ribosyl) transferase. Biochem Biophys Res Commun. 1997;240:108–11.

Oliver FJ, Menissier-de Murcia J, Nacci C, Decker P, Andriantsitohaina R, Muller S, et al. Resistance to endotoxic shock as a consequence of defective NF-kappaB activation in poly (ADP-ribose) polymerase-1 deficient mice. Embo J. 1999;18:4446–54.

Ravi R, Bedi GC, Engstrom LW, Zeng Q, Mookerjee B, Gelinas C, et al. Regulation of death receptor expression and TRAIL/Apo2L-induced apoptosis by NF-kappaB. Nat Cell Biol. 2001;3:409–16.

Realini CA, Althaus FR. Histone shuttling by poly(ADP-ribosylation). J Biol Chem. 1992;267:18858–65.

Ryan KM, Ernst MK, Rice NR, Vousden KH. Role of NF-kappaB in p53-mediated programmed cell death. Nature 2000;404:892–7.

Schreiber V, Dantzer F, Ame JC, de Murcia G. Poly(ADP-ribose): novel functions for an old molecule. Nat Rev Mol Cell Biol. 2006;7:517–28.

Soldatenkov VA, Chasovskikh S, Potaman VN, Trofimova I, Smulson ME, Dritschilo A. Transcriptional repression by binding of poly(ADP-ribose) polymerase to promoter sequences. J Biol Chem. 2002;277:665–70.

Thome M, Martinon F, Hofmann K, Rubio V, Steiner V, Schneider P, et al. Equine herpesvirus-2 E10 gene product, but not its cellular homologue, activates NF-kappaB transcription factor and c-Jun N-terminal kinase. J Biol Chem. 1999;274:9962–8.

Tulin A, Spradling A. Chromatin loosening by poly(ADP)-ribose polymerase (PARP) at *Drosophila* puff loci. Science 2003;299:560–2.

Van Antwerp DJ, Martin SJ, Kafri T, Green DR, Verma IM. Suppression of TNF-alpha-induced apoptosis by NF-kappaB. Science 1996;274:787–9.

Vandesompele J, De Preter K, Pattyn F, Poppe B, Van Roy N, De Paepe A, et al. Accurate normalization of real-time quantitative RT-PCR data by geometric averaging of multiple internal control genes. Genome Biol. 2002;3:1–12.

Wesierska-Gadek J, Wojciechowski J, Schmid G. Phosphorylation regulates the interaction and complex formation between wt p53 protein and PARP-1. J Cell Biochem. 2003;89:1260–84.

Willis TG, Jadayel DM, Du MQ, Peng H, Perry AR, Abdul-Rauf M, et al. Bcl10 is involved in t(1;14)(p22;q32) of MALT B cell lymphoma and mutated in multiple tumor types. Cell 1999;96:35–45.

Yan M, Lee J, Schilbach S, Goddard A, Dixit V. mE10, a novel caspase recruitment domain-containing proapoptotic molecule. J Biol Chem. 1999;274:10287–92.

Zhang Z, Hildebrandt EF, Simbulan-Rosenthal CM, Anderson MG. Sequence-specific binding of poly(ADP-ribose) polymerase-1 to the human T cell leukemia virus type-I tax responsive element. Virology 2002;296:107–16.